Modelling and LQR robust control of an unmanned aerial vehicle for air-launch

van Cuong Nguyen, Gilney Damm, Naoufel Azouz, Claire Vasiljevic, Etienne Colle

Modeling and LQR robust control of an unmanned aerial vehicle for airlaunch

Van Cuong Nguyen and Gilney Damm and Naoufel Azouz and Claire Vasiljevic and Etienne Colle

***Abstract*— A satellite launching procedure known as airlaunch is modeled and simulated at the staging phase, where a reusable unmanned aerial vehicle air-launches a second (rocket) stage. Airlaunch is described by the variations in mass, inertia and aerodynamic coefficients of airlaunch system and their effects on the stability of the airlaunch system at the stage separation. In this paper, this procedure may imply on large variation in angle of attack, sideslip and roll angle of the airlaunch system caused by perturbations on aerodynamic forces and moments during the launch phase. In order to stand these perturbations, it is proposed an LQR controller obtained by optimal and robust control theory. This controller is designed with the objective of stabilizing the system after the airlaunch. Performance of the proposed control algorithm is illustrated through computer simulations.**

I. Introduction

Satellites launching is a strategical activity today. Launchers are able to carry from micro-satellites of some tens of kilograms up to 10 tons in the case of French Ariane 5 launcher. Recently new applications have called upon very small satellites, named nano-satellites, mostly used in groups (see [1]). These nano-satellites need a new class of launchers since launching implies in many fixed costs that are independent of the size and weight of the launched device. For this reason, the ratio price-per-kilogram launched in space becomes too high. A quite logical solution in this case would be to pack many small devices to be launched together. Unfortunately this implies many additional risks in the split phase and is not envisaged.

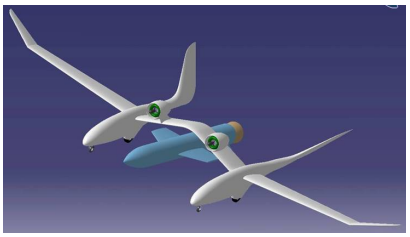

Fig. 1. An airlauch system

Van Cuong Nguyen is with IBISC - Université d'Evry Val d'Essonne, Evry, France vancuong.nguyen@ibisc.fr

Gilney Damm is with IBISC - Université d'Evry Val d'Essonne, Evry, France gilney.damm@ibisc.fr

Naoufel Azouz is with IBISC - Université d'Evry Val d'Essonne, Evry, France naoufel.azouz@ibisc.fr

Claire Vasiljevic is with IBISC - Université d'Evry Val d'Essonne, Evry, France claire.vasiljevic@ibisc.fr

Etienne Colle is with IBISC - Université d'Evry Val d'Essonne, Evry, France etienne.colle@ibisc.fr

A more efficient solution in this case is to use the procedure of airlaunch (see [8], [3]). It consists of using a two stages launching system (see Fig. 1). The first stage is composed of an air vehicle (manned or unmanned) that carries (inside, beneath or above) a launcher which constitutes the second stage. There are many advantages in airlaunch, mainly because there is no need for specific large non populated launching areas. The aerial vehicle takes-off from a standard runway and fly to open ocean, avoiding populated areas or ship and airplane paths. For this reason there is also a minimization of weather constraints, since the vehicle can fly to open sky, and as consequence the launch delay can be significantly shortened. Similarly, instead of waiting for specific launch windows (to attain desired orbits), the vehicle may be flown to a better suited launch point, with a better alignment with the desired orbit. The fact that the first stage is a reusable aerial vehicle allows a much smaller launching delay. In the same way, launching reuse time may be very short (one or two days). These characteristics provide great flexibility, and allow to deploy small satellites designed for specific tasks of communication or data gathering in real time for urgent situations.

Airlaunch provides the advantages of two stage launchers. The second (dropped) stage may use specific nozzles and propellants for the low outside atmospheric pressure at altitude (20000 meters or 60000 feet). This is obtained without the complex, expensive and relatively dangerous high pressure ground-launched first stage that is replaced by the aerial vehicle. Most current airlaunch projects use standard or lightly modified airplanes as first stage. For example, there has been tests using F15, C17, B52, L-1011 in Rascal, QuickReach, Proteus and Pegasus projects.

It is important to remark that airplanes use the wing's lift force to fly. For this reason, higher (low altitude) air density benefit the flight while the aircraft uses standard fuel to keep flying. A first stage rocket would use a much more complex, dangerous and expensive fuel while in this higher air density. From a certain altitude, air density is too low to be useful for an airplane, while not representing anymore a drawback for rockets.

For all these reasons some projects are currently developing airlaunch strategies, where some of them intends to use an unmanned aerial vehicle to fly the launcher to the desired drop point. There are many advantages in doing so, in first place safety since no human lives are involved during the delicate launching phase. In addition, since there is no need for life supporting devices, weight is restricted to the strict minimum. Finally, mission may take as long as necessary

without human restrictions as tiredness.

The present paper consider an airlaunch system that uses an Unmanned Aerial Vehicle (UAV) instead of a standard aircraft with a human pilot inboard, and addresses the launching phase. It intends to introduce modeling and a robust controller for this delicate procedure. In fact, airlaunch may be very challenging since the rocket may be almost as heavy as the UAV. This means that the aircraft will instantaneously lose almost half of its mass. Current airlaunch systems present a much smaller ratio launcher/aircraft and rely on human pilot to stabilize the aircraft during and immediately after the launching instant. Unlike those systems, this airlaunch uses an UAV, and as consequence, the stabilization task is much more complex during and after the launching phase with a much more adverse mass ratio. To the best of our knowledge, it does not exist an equivalent research line, and then there is no results in the literature considering this problem (modeling and control).

The paper is organized as follows: in section II-C, we describe the nonlinear mathematical system model, two approaches of airlaunch phase are also presented in this section. A LQR control design is discussed in section III, and its application to the full system model. The paper is completed by computer simulations and conclusions.

II. Modeling

The airlaunch phase can be described by the variations in mass, inertia and aerodynamic coefficients of airlaunch system before and after launch phase. Modeling this phase requires a large amount of data and previous knowledge about the real system, which is actually not available in the case of study. However, it can also be represented as a hybrid system composed by two (or three) continuous models that are switched. These models represents the system before, (possible during) and after the separation phase. In the present work we have adopted this strategy, we have considered three phases.

1) before the separation $\Rightarrow$ a first aircraft model (representing the UAV and the rocket) is in an stable operating condition
2) during the separation $\Rightarrow$ a second aircraft model representing only the UAV, starting on the previous operating condition is disturbed by impulses on forces and moments. These disturbances are inside a time interval T_{int} and represent a not perfect separation. Furthermore the initial conditions, inherited from the first phase, are not an equilibrium point for the second aircraft model.
3) after the separation $\Rightarrow$ the disturbances stop (UAV and rocket are not in physical contact anymore). It can be shown that the effect of launching the rocket from the UAV impacts most the lift force, and the roll and pitch moments.

From this strategy, we have two approaches to model the airlaunch phase that we present in the following section.

A. Initial Condition Approach

As a first approach to model the system, we adopt a hybrid technique that considers the airlaunch as a switch between two continuous models, one previous the launch phase and one following it. The switch itself is considered as instantaneous, but imperfect. In this way impulses in forces and moments affect the aircraft, resulting in possibly large initial conditions for the second model, which is taken as an F-16. The resulting control task may be stated as to design an stabilizing controller for this second system (after the switch) with possible large initial conditions.

B. Perturbation on aerodynamic force and moment approach

In a second approach to model our system, we have also considered the airlaunch as a switch between two continuous models:

1) before the separation $\Rightarrow$ the first model is considered at an stable operating condition
2) during the separation $\Rightarrow$ the launch phase itself happens during an interval T_{int}. During this interval the second model is used, but disturbed by constant aerodynamic force and moment modeling an imperfect launching of the rocket from the aircraft
3) after the separation $\Rightarrow$ the disturbances stop, and the second model continues to be used

In order to make our study as much general as possible, the first model is taken as an F-16 with twice its normal mass, while the second model is taken as the complete F-16 model.

It can be shown that the effect of launching the rocket from the flight disturb mostly lift force and pitch and roll moments. We suppose that these disturbing force and moments are constant during the interval T_{int}. We call F_{z_p}, L_p and M_p the disturbances on the lift force, on the roll moment and pitch moment respectively.

We suppose that:

- the perturbation on lift force during T_{int} is equal to the rocket's mass, that means $F_z = mg$.
- the perturbation on pitch moment during T_{int} is an worst case that is represented by the rocket that remains attached to the aircraft by only one end during T_{int}, applying a rotational movement to the aircraft, so a moment with value $F_z = mgl_r/2$ where l_r is the rocket length.
- the perturbation on roll moment during T_{int} is small because of the rocket shape (long and thin).
- the model following the launch phase is the F-16 model. Its initial condition is the state at an equilibrium point of the model previous the launch phase that is the F-16 model but with twice its standard mass.

C. System Model

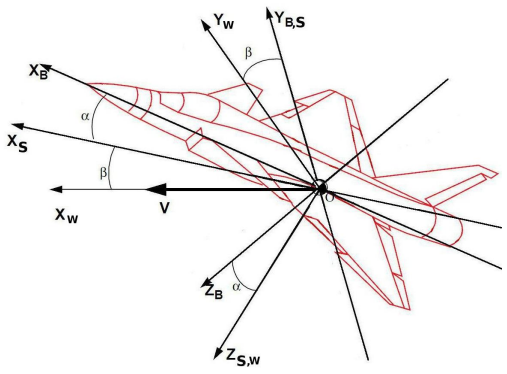

Fig. 2. Frames: Body fixed axes $OX_BY_BZ_B$, Stability axes $OX_SY_SZ_S$, Aerodynamic axes $OX_WY_WZ_W$

Following this procedure, the F-16 aircraft in the instant following the dynamic airlaunch is described in the body fixed axes as (see [2], [10], [12]).

$$\left\{\begin{array}{l}\dot{u} = rv - qw - g\sin\theta + \frac{1}{m}(F_x + T)\\ \dot{v} = pw - ru + g\sin\phi\cos\theta + \frac{1}{m}F_y\\ \dot{w} = qu - pv + g\cos\phi\cos\theta + \frac{1}{m}F_z\\ \dot{p} = \frac{1}{I_{xx}I_{zz} - I_{xz}^2}[(I_{yy}I_{zz} - I_{zz}^2 - I_{xz}^2)rq - I_{xz}(I_{xx}\\ +I_{zz} - I_{yy})pq + I_{zz}L - I_{xz}N]\\ \dot{q} = \frac{1}{I_{yy}}[(I_{zz} - I_{xx})pr + I_{xz}(p^2 - r^2) + M]\\ \dot{r} = \frac{1}{I_{xx}I_{zz} - I_{xz}^2}[(-I_{xx}I_{yy} + I_{zz}^2 + I_{xz}^2)pq\\ +I_{xz}(I_{xx} + I_{zz} - I_{yy})rq + I_{xx}N - I_{xz}L]\\ \dot{\phi} = p + \tan\theta(q\sin\phi + r\cos\phi)\\ \dot{\theta} = q\cos\phi - r\sin\phi\\ \dot{\psi} = \frac{q\sin\phi + r\cos\phi}{\cos\theta}\end{array}\right\} \quad (1)$$

In addition we use state variables in the aerodynamic axes (the aerodynamic axes $OX_WY_WZ_W$ in the Fig. 2) i.e. the reference frame attached to the airspeed vector (V) instead of using variables in body fixed axes because of the measurability of these state variables, we then rewrite the system into the aerodynamic axes as in (2).

In (1) and (2), $I_{xx}, I_{yy}, I_{zz}, I_{xz}$ are the moments of inertia, m is the mass of the system (kg) and g the gravity constant.u, v, w are translational velocities of the system in body fixed axes in m/s. $\alpha, \beta, V, p, q, r, \phi, \theta, \psi$ are the state variables of the airlaunch aircraft model, they are the angle of attack, sideslip, airspeed, roll rate, pitch rate, yaw rate, roll angle, pitch angle and yaw angle respectively. $\alpha, \beta, \phi, \theta, \psi$ are expressed in rad, p, q, r in rad/s and V in m/s. T is the thrust force, F_x, F_y, F_z and L, M, N are aerodynamic forces and moments respectively. All forces and moments are expressed in N and Nm.

$$\left\{\begin{array}{l}\dot{\alpha} = -\cos\alpha\tan\beta p + q - \sin\alpha\tan\beta r\\ -\frac{\sin\alpha}{mV\cos\beta}(T + F_x) + \frac{\cos\alpha}{mV\cos\beta}F_z\\ +\frac{g}{V\cos\beta}[\sin\alpha\cos\theta + \cos\alpha\cos\phi\cos\theta]\\ \dot{\beta} = \sin\alpha p - \cos\alpha r - \frac{\cos\alpha\sin\beta}{mV}[T + F_x] + \frac{\cos\beta}{mV}F_y\\ -\frac{\sin\alpha\sin\beta}{mV}F_z + \frac{g}{V}[\cos\alpha\sin\beta\sin\theta\\ +\cos\beta\cos\theta\sin\phi - \sin\alpha\sin\beta\cos\phi\cos\theta]\\ \dot{V} = \frac{\cos\alpha\cos\beta}{m}[T + F_x] + \frac{\sin\beta}{m}F_y\\ +\frac{\sin\alpha\cos\beta}{m}F_z + g[\cos\alpha\cos\beta\sin\theta\\ +\sin\beta\sin\phi\cos\theta + \sin\alpha\cos\beta\cos\phi\cos\theta]\\ \dot{p} = \frac{1}{I_{xx}I_{zz} - I_{xz}^2}[(I_{yy}I_{zz} - I_{zz}^2 - I_{xz}^2)rq - I_{xz}(I_{xx}\\ +I_{zz} - I_{yy})pq + I_{zz}L - I_{xz}N]\\ \dot{q} = \frac{1}{I_{yy}}[(I_{zz} - I_{xx})pr + I_{xz}(p^2 - r^2) + M]\\ \dot{r} = \frac{1}{I_{xx}I_{zz} - I_{xz}^2}[(-I_{xx}I_{yy} + I_{zz}^2 + I_{xz}^2)pq\\ +I_{xz}(I_{xx} + I_{zz} - I_{yy})rq + I_{xx}N - I_{xz}L]\\ \dot{\phi} = p + \tan\theta(q\sin\phi + r\cos\phi)\\ \dot{\theta} = q\cos\phi - r\sin\phi\\ \dot{\psi} = \frac{q\sin\phi + r\cos\phi}{\cos\theta}\end{array}\right\} \quad (2)$$

These aerodynamic forces and moments are function of all the considered states. In this model, these aerodynamic forces and moments are under look-up table from wind tunnel data measurements as may be found in [6]. Finally, the control inputs are respectively the aileron (δ_a), rudder (δ_r) and elevator (δ_e) angles.

This model is based on wind tunnel data from NASA, considering the following conditions:

- angle of attack is in the range of $[-10°, 45°]$ and sideslip of $[-30°, 30°]$
- flag deflection is ignored
- physical constraints for aileron ($|\delta_a| \leq 21.5°$), rudders ($|\delta_e| \leq 25°$) and elevator ($|\delta_r| \leq 30°$)
- all actuators are modeled as a first order model ($\tau = 1/0.0495s$) with limit rates $60°/s$ for aileron and elevator, and $120°/s$ for rudder.

In particular, we use the low quality mode of the F-16 model, and the aerodynamic data is interpolated and extrapolated linearly in simulation from tables found in [6].

III. LQR CONTROL

A consequence of the considered model is that the control design for the airlaunch phase becomes more difficult because this is a nonlinear model and its aerodynamic coefficients are under tabular form that requires the interpolation and extrapolation for the aerodynamic coefficients values.

There exist some approaches for controlling this class of systems like in [9] based on sliding mode control, and [7] and [4]) where it was applied backstepping control techniques. In the present work, our control approach is based on a optimal robust LQR control. The controller will be presented in the following section and its results will be illustrated by simulations.

A. LQR control design

The equations of the system in (2) can be rewritten under general form removing the differential equation of airspeed

which has a slower dynamic than the other states:

$$\left\{ \begin{array}{l} \dot{x} = f(x,u) \\ y = Cx \end{array} \right\} \tag{3}$$

Where $x = (\alpha, \beta, p, q, r, \phi, \theta, \psi)^T$ is the state, the output is $y = (\alpha, \beta, \phi)^T$ and the input is represented by $u = (\delta_a, \delta_e, \delta_r)^T$. Our objective is to design a controller $u = (\delta_a, \delta_e, \delta_r)$ such that the output $y = (\alpha, \beta, \phi)^T$ is asymptoticly stabilized to the desired reference output $y_r = (\alpha_r, \beta_r, \phi_r)^T$. Our LQR control approach is based on the linearization around an equilibrium point (also called an operating point) of the system. In order to linearize the system (3), we make the following assumption:

Assumption: Given a desired operating point $(\bar{V}, \bar{h}$ corresponding to airspeed and altitude of the system, there exists an unique input $\bar{u}$ and state $\bar{x}$ so that $f(\bar{x}, \bar{u}) = 0$.

Defining the input error, state error and output error respectively by : $\tilde{u} = u - \bar{u}$, $\tilde{x} = x - \bar{x}$, $\tilde{y} = y - \bar{y}$, the linear approximation of (3) can be expressed as:

$$\left\{ \begin{array}{l} \dot{\tilde{x}} = A\tilde{x} + B\tilde{u} \\ \tilde{y} = C\tilde{x} \end{array} \right\} \tag{4}$$

Where $A = \frac{\partial f(\bar{x},\bar{u})}{\partial x}$, $B = \frac{\partial f(\bar{x},\bar{u})}{\partial u}$, $C = \begin{bmatrix} 1 & 0 & 0 & 0 & 0 & 0 & 0 & 0 \\ 0 & 1 & 0 & 0 & 0 & 0 & 0 & 0 \\ 0 & 0 & 0 & 0 & 0 & 1 & 0 & 0 \end{bmatrix}$.

If (A, B) is stabilizable, and for $Q \in \mathbb{R}^{8\times 8}$ positive definite, $R \in \mathbb{R}^{3\times 3}$ positive semidefinite, the LQR control law has the form (see [5],[11]):

$$\tilde{u} = -K\tilde{x} \tag{5}$$

Where $K = R^{-1}BP$, with P the positive semidefinite solution of the Riccati equation:

$$A^T P + PA + Q - PBR^{-1}B^T P = 0 \tag{6}$$

IV. Simulation and Results

In the following simulations, we have applied the LQR control for stabilizing all states of the second model to its equilibrium point from several initial conditions in the first modeling approach and from disturbances on aerodynamic force and moment for the second modeling approach. This illustrates the performance of the LQR control face to several launch conditions. Our control task is to:

- stabilize the states of the second model to its equilibrium point, which is is considered on the operating point $(V, h) = (154m/s, 6500m)$ corresponding to the trimmed angle of attack $\alpha_0 = 2.7°$, pitch angle $\theta_0 = 2.7°$ sideslip $\beta_0 = 0°$ and $\phi_0 = 0°$ and to trimmed control surface states: aileron $\delta_a = 0°$, elevator $\delta_e = -2.0°$ and rudder $\delta_r = 0°$.
- guarantee the physical limitations of the actuators ($|\delta_a| < 21.5°$, $|\delta_e| < 25°$ and $|\delta_r| < 30°$).
- assure the flighting field of the F-16 model:
  - limit rates $60°/s$ for pitch and yaw rates, and $90°/s$ for roll rate.
  - limit angles $|360°|$ for roll and yaw angles and $|90°|$ for pitch angle.

The parameter of the controller $\tilde{u} = -K\tilde{x}$ is:

$$K = \begin{bmatrix} -0.2 & 29.4 & -11.2 & -0.2 & -7.7 & -13.7 & -0.0 & -0.4 \\ 0.7 & -1.9 & 0.3 & -38.3 & 0.0 & 0.3 & -1.0 & 0.0 \\ -0.2 & 0.6 & 1.9 & -0.1 & -12.4 & 1.4 & -0.0 & -0.1 \end{bmatrix} \tag{7}$$

In order to control airspeed, we design a simple PI controller for the thrust to regulate the airspeed of the system. Its form is:

$$T = -k_P(V - V_{ref}) - k_I(\dot{V} - \dot{V}_{ref})$$

where V_{ref} is airspeed at the equilibrium point of the second model, $k_P = 1242$ and $k_I = 955$.

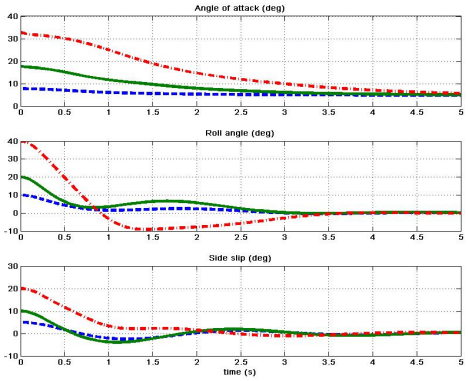

Fig. 3. Outputs stability: Angle of attack α, sideslip β and roll angle ϕ stabilized

A. Initial Condition Approach

As explained in section (II-A), this approach only uses the second model. The separation phase results in large initial conditions in respect to the equilibrium point (angle of attack $\alpha = 2.7°$, sideslip angle $\beta = 0°$ and roll angle $\phi = 0°$) on the second model, which is an F-16 model.

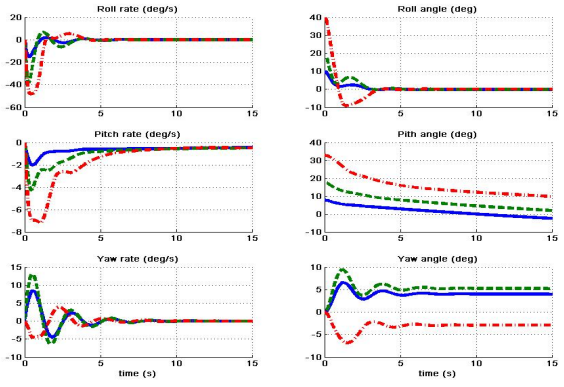

Fig. 4. States Stability: angular rates and Euler's angles

For our study, we consider three sets of initial conditions. First case corresponds to a small initial condition error from the trimmed ones of the aircraft after the phase of drop stage,

with an angle of attack $\alpha = 7.7°$, sideslip $\beta = 5°$ and roll angle $\phi = 10°$.

The second case is a medium error between the initial and trimmed conditions with $\alpha = 17.7°$, sideslip $\beta = 10°$ and $\phi = 20°$. The last case corresponds to a large initial condition with $\alpha = 32.7°$, sideslip $\beta = 20°$ and $\phi = 40°$. In the following, one may see how the system responds to these three cases.

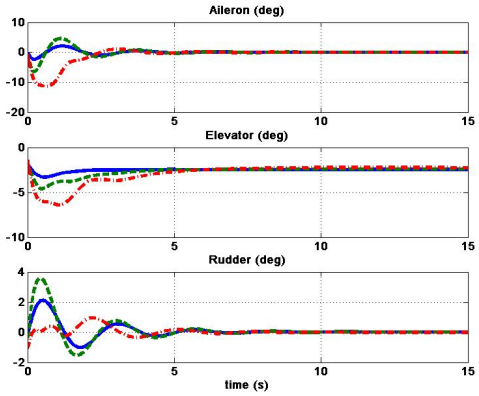

Fig. 5. Control surfaces: aileron δ_a, elevator δ_e and rudder δ_a controls

Fig. 3 shows the convergence of the controlled outputs with the LQR controller for different initial conditions, in the three cases distinct from trimmed conditions. The dashed black line indicates the controlled outputs of system in the first case, the continuous line is the controlled outputs for an medium error case, and the large error situation corresponds to the dash dotted line.

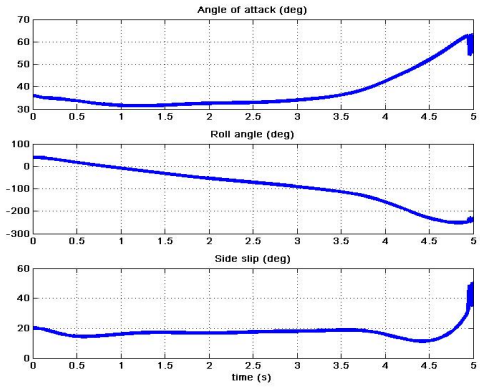

Fig. 6. Outputs stability: Angle of attack α, sideslip β and roll angle ϕ stabilized

Fig. 4 represents the behavior of other states of the system. In the left side, one can see that the angular rates return to the origin. In the right side, it is shown how Euler's angles converge. The yaw angle that illustrates the lateral motion, can be free, but in this case it is stabilized. In Fig. 5 it is illustrated the input controls for the three studied cases.

In these three cases of study, the outputs are stabilized to the operating point values. This illustrates the good performance of the LQR controller. It can be easily seen that the outputs return quickly to the operating point in $5s$. This is compatible to the desired specification. In terms of control inputs in Fig. 5, all actuators are inside their bounds for the three cases, i.e. inside the limits of $21.5°$ for ailerons δ_a, $25°$ for elevators δ_e and of $30°$ for rudders δ_r.

To verify the impact of very large errors on the initial conditions in the drop phase, we increase them to: angle of attack $\alpha = 35°$, sideslip $\beta = 20°$ and $\phi = 40°$. The simulation result is demonstrated in Fig. 6 for the controlled outputs and in Fig. 7 for the control surfaces.

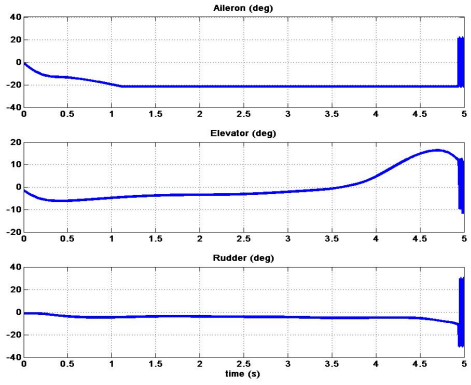

Fig. 7. Angle of attack α, sideslip β and roll angle ϕ stabilized

Fig. 6 shows that the state outputs become unstable, the roll angle is out of the flighting range of the F-16 model. In Fig. 7 it is shown that the demanded surface controls are very high compared to their physical limitations. The response of the system in this case is not compatible to the required specification and flighting range of the F-16 model. It is possible that, since control inputs are saturated, this illustrates the physical limits of stabilizability of this kind of aircraft, independently of the applied control strategy.

B. Approach of perturbation on aerodynamic force and moment

We consider now the modeling approach of the airlaunch phase studied in subsection II-B. In a first step, the airlaunch system s taken with constant control inputs. We can then find a maximum time interval T_{Max} beyond which the disturbances affecting aerodynamic force and moment bring the system unstable. In a second step, we show that the LQR controller designed in (III-A) will stabilize the airlaunch system for several intervals T_{int} greater than T_{Max}.

We take, as the initial condition of the second model, an equilibrium point of the first model that is the F-16 model but with double F-16's mass. The operating point is $(V, h) = (154m/s, 6500m)$, that corresponds to the trimmed angle of attack $\alpha_0 = 12.5°$, pitch angle $\theta_0 = 12.5°$ sideslip $\beta_0 = 0°$, $\phi_0 = 0°$ and to control surface states: aileron $\delta_a = 0°$, elevator $\delta_e = -4.0°$ and rudder $\delta_r = 0°$.

The second model following the launch phase will be stabilized to its equilibrium point $(V, h) = (154m/s, 6500m)$, that means angle of attack α_0 to $2.7°$, sideslip β to $0°$, and roll angle ϕ to $0°$.

1) Airlaunch system without LQR Controller: At first, we take an interval of perturbation $T_{int} = 0.2s$, the simulation of model can be seen in Fig. 8. The angle of attack and the sideslip seem to be stabilized to perturbation on aerodynamic force and moment. However, Fig. 9 shows that roll angle and pitch angle are not stabilized. The system becomes then unstable for the perturbation on aerodynamic force and moment during $T_{int} = 0.2s$.

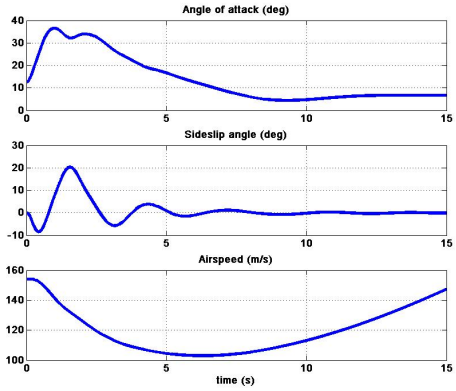

Fig. 8. Angle of attack α, Sideslip β and Airspeed V

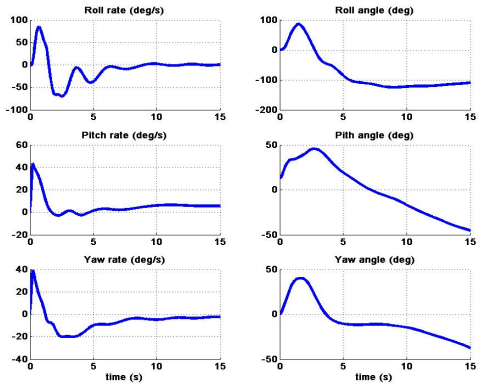

Fig. 9. Outputs stability: Angular Rates and Euler's Angles

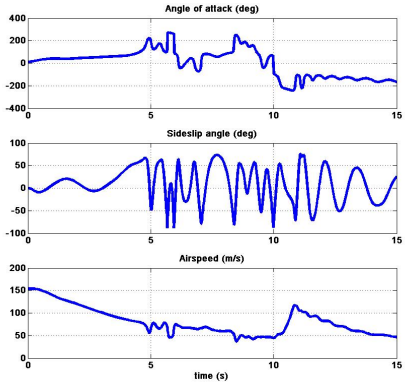

Fig. 10. Instability of Angle of attack, Sideslip and Airspeed

In order to see more clearly the instability of the second model affected by the perturbation, we increase T_{int} to $0.227s$, the system will be completely unstable as shown in Fig. 10. The value of T_{Max} is then $0.227s$. A control system is then needed to stabilize the airlaunch system after the launch phase.

2) Airlaunch system with LQR Controller: The LQR designed in subsection III-A is applied to airlaunch system in order to stabilize the system states after the launch phase. To this purpose, we are interested in the stability of angle of attack, sideslip, roll angle, pitch angle, roll rate, pitch rate and yaw rate. The yaw angle, that illustrates the lateral motion, can be neglected in this study.

We make the simulations using two disturbance durations, $T_{int} = 0.2227s$ that made the airlaunch with constant control inputs unstable, and $T_{int} = 0.3s$ that will show the limits of the proposed control scheme. For the simulation procedure, we take the worst case perturbation described in subsection II-B.

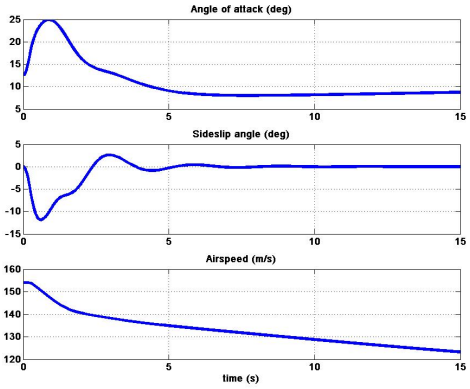

Fig. 11. Angle of attack α, sideslip β stabilized

Figs. 11 to 13 show the simulation of airlaunch system controlled by LQR control with perturbation during $T_{int} = 0.2227s$. The desired system outputs are angle of attack, sideslip and roll angle which are stabilized by LQR control to the equilibrium point of the model following the launch phase (see Fig. 11 and Fig. 12).

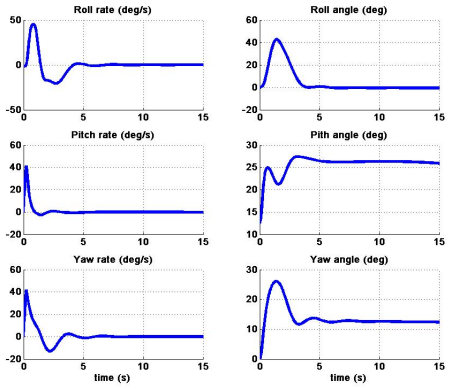

Fig. 12. Angular rates and Euler's angles stabilized

Fig. 12 also shows the convergence to zero of angular rates of the system after launch phase. Control surfaces seen in Fig. 13 are always in their physical limitations. The result

from Fig. 11 to Fig. 13 shows that the airlaunch system is stabilized by the LQR controller.

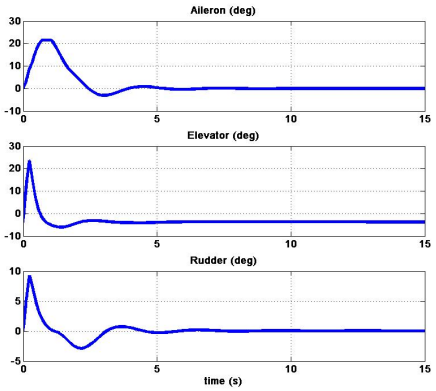

Fig. 13. Aileron δ_a, Elevator δ_e and Rudder δ_a

When the perturbation T_{int} becomes too long, the airlaunch system can not remain stable even with the LQR controller. Fig. 14 shows the system becomes unstable because of long perturbation time on aerodynamic force and moment. The control surfaces in this case are saturated by their physical limitations (see in Fig. 15).

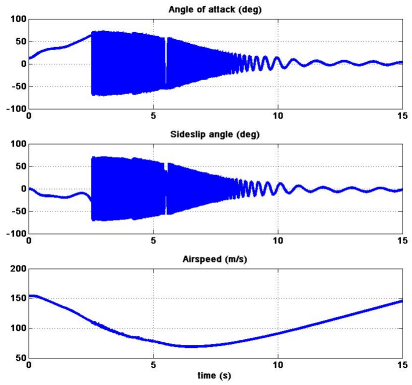

Fig. 14. Angle of attack α, Sideslip β unstable

V. Conclusion

We have introduced the modeling and simulation of an airlaunch system at the stage separation from a reusable airlaunch vehicle from the down stage. This work allows to illustrate the effects of the variations in mass, inertia, and aerodynamic coefficients at the staging phase in the stability of the airlaunch system. Because our airlaunch system have a down stage mass close to the launch vehicle's one, the separation phase produces large changes in the angle of attack, sideslip and other states of the system in a first modeling approach and large changes in aerodynamic force and moment for a second modeling approach of airlaunch phase, as demonstrated in section II-C, which may bring the system unstable.

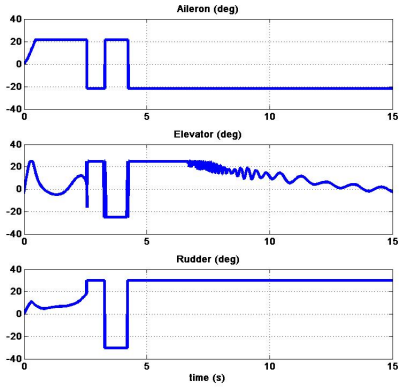

Fig. 15. Aileron δ_a, Elevator δ_e and Rudder δ_a saturated

The first approach to model the airlaunch phase based on initial conditions is simpler, but less complete, mainly because we can not study all initial conditions of system's states in the required flight envelop. The second approach based on perturbation on aerodynamic force and moment of the airlaunch system represents the continuity of the effect of airlaunch on the second model and is a better choice for modeling the airlaunch phase. It has also the advantage of allowing simulation of proposed controllers during the disturbance itself, such as to evaluate the ability of the controller to attenuate the effects of these disturbances.

To stabilize the airlaunch system after this stage separation phase, an LQR control is designed using optimal robust control theory. This controller is made using an F-16 model representing the aircraft just after dropping the second stage.

In the modeling approach based on an initial condition different from the equilibrium point, the effects of the proposed controller are illustrated in computer simulations with several initial conditions distinct from the equilibrium. In the case of small error on initial conditions, the stability of the system after the drop stage is assured. When the error becomes large, the state outputs are poorly stabilized causing bad transients. This can either illustrate the limitations of the proposed controller or the limitations of the aircraft itself.

In the second modeling approach applying disturbances on aerodynamic force and moment, the stability of the system after the drop stage is assured even in an worst case when the disturbance does not last too long. When the disturbance lasts longer, the state outputs become unstable. Since inputs saturate, this could also happen for other control schemes and would represent physical limitations.

In future works both possibilities will be explored (limitations from the control scheme or from the aircraft) as well as to study other control strategies for this particularly interesting and difficult problem. The objective being to perform flight tests in a near future with small scaled models. In the same way, we expect wind tunnel tests with the UAV under construction, to provide a suitable model of the system before and after airlaunch. The present results will then be adapted to this new model, but already with the benefit of the current conclusions.

REFERENCES

[1] M.M. Burlacu and J. Kohlenberg. An analysis of the nanosatellites launches between 2004 and 2007. *3rd International Conference on Systems and Networks Communications*, pages 292–297, 2008.

[2] Thor I. Fossen. *Guidance and Control of Ocean Vehicles*. Wiley, 1994.

[3] Gary C. Hudson. Quickreach responsive launch system. *American Institute of Aeronautics and Astronautics*, 2006.

[4] Taeyoung Lee and Youdan Kim. Nonlinear adaptive flight control using backstepping and neural networks controller. *Journal of guidance, control and dynamics*, 24:675–682, 2001.

[5] J.-F. Magni, S. Bennani, and J.Terlouw. *Robust Flight Control : A Design Challenge*. Springer, 1997.

[6] L.T. Nguyen, M.E. Ogburn, and P. Deal. Simulator study of fighter airplane with relaxed longitudinal static stability. *Technical report NASA*, page 1538, 1979.

[7] JohnW.C. Robinson. Block backstepping for nonlinear flight control law design. *Springer*, page 231257, 2007.

[8] Marti Sarigul-Klijn and Nesrin Sarigul-Klijn. Selection of a carrier aircraft and a launch method for air launching space vehicles. *American Institute of Aeronautics and Astronautics*, 2008.

[9] Sridhar Seshagiri and Ekprasit Promtun. Sliding mode control of f-16 longitudinal dynamics. *American Control Conference*, pages 1770–1775, 2008.

[10] Lars Sonneveldt. *Nonlinear F-16 Model Description*. Delft University of Technology, Netherlands, 2006.

[11] Emmanuel Trlat. *Commande optimale*. Notes du cours A08, 2008.

[12] Peter H. Zipfel. *Modeling and Simulation of Aerospace Vehicle Dynamics, 2nd edition*. American Institute of Aeronautics and Astronautics, 2000.